EPJ Plus

EPJ.org
your physics journal

Eur. Phys. J. Plus (2017) **132**: 289 DOI 10.1140/epjp/i2017-11543-4

Models for the transient stability of conventional power generating stations connected to low inertia systems

Marios Zarifakis, William T. Coffey, Yuri P. Kalmykov and Sergei V. Titov

Società Italiana di Fisica

Springer

Eur. Phys. J. Plus (2017) **132**: 289
DOI 10.1140/epjp/i2017-11543-4

THE EUROPEAN PHYSICAL JOURNAL PLUS

Regular Article

Models for the transient stability of conventional power generating stations connected to low inertia systems*

Marios Zarifakis[1,2,a], William T. Coffey[2], Yuri P. Kalmykov[3], and Sergei V. Titov[4]

[1] Electricity Supply Board, Generation, Asset Management, Dublin 2, Ireland
[2] Department of Electronic and Electrical Engineering, Trinity College, Dublin 2, Ireland
[3] Laboratoire de Mathématiques et Physique (EA 4217), Université de Perpignan Via Domitia, F-66860, Perpignan, France
[4] Kotel'nikov Institute of Radio Engineering and Electronics of the Russian Academy of Sciences, Vvedenskii Square 1, Fryazino, Moscow Region, 141120, Russia

Received: 1 December 2016 / Revised: 9 May 2017
Published online: 30 June 2017 –

Abstract. An ever-increasing requirement to integrate greater amounts of electrical energy from renewable sources especially from wind turbines and solar photo-voltaic installations exists and recent experience in the island of Ireland demonstrates that this requirement influences the behaviour of conventional generating stations. One observation is the change in the electrical power output of synchronous generators following a transient disturbance especially their oscillatory behaviour accompanied by similar oscillatory behaviour of the grid frequency, both becoming more pronounced with reducing grid inertia. This behaviour cannot be reproduced with existing mathematical models indicating that an understanding of the behaviour of synchronous generators, subjected to various disturbances especially in a system with low inertia requires a new modelling technique. Thus two models of a generating station based on a double pendulum described by a system of coupled nonlinear differential equations and suitable for analysis of its stability corresponding to infinite or finite grid inertia are presented. Formal analytic solutions of the equations of motion are given and compared with numerical solutions. In particular the new finite grid model will allow one to identify limitations to the operational range of the synchronous generators used in conventional power generation and also to identify limits, such as the allowable Rate of Change of Frequency which is currently set to $\pm 0.5\,\mathrm{Hz/s}$ and is a major factor in describing the volatility of a grid as well as identifying requirements to the total inertia necessary, which is currently provided by conventional power generators only, thus allowing one to maximise the usage of grid connected non-synchronous generators, *e.g.*, wind turbines and solar photo-voltaic installations.

1 Introduction

The requirement to decarbonize electrical energy production is leading to an increase of wind turbine and solar photo-voltaic based energy generation. These renewable generation sources in comparison to conventional *synchronously* grid connected turbo generators of gas, oil or even coal fired power stations are *asynchronously* connected to the grid. Inadvertently, by increasing the extent of asynchronously grid connected generation the stability of the entire electricity network is reduced thereby also affecting the existing conventional power generation units. Examples are the increase of electrical power oscillations of conventional power generating units and also consequential tripping of some larger units which occur during transient events at times of high wind generation in the system. In addition certain transient events like a sudden generation to load imbalance which arises after a trip of a generating unit, a disconnection of a large load or during a system separation event manifest themselves in a grid frequency drop, rise or even oscillation. The weakening of the grid frequency strength manifests itself via an increase of the Rate of Change of Frequency (ROCOF). Historically, the ROCOF was limited by the manufacturers of conventional generating units to $\pm 0.5\,\mathrm{Hz/s}$ suggesting that an increase in excess of this value needs to be analysed especially in relation to the manufacturer's specification thereby allowing for a further increase of non-synchronously connected electrical generation sources like wind turbine generators and solar PV installations. Now to enable one to initially quantify the influence of more severe ROCOF events on the

* Contribution to the Focus Point on "The Transition to Sustainable Energy Systems" edited by J. Ongena.

[a] e-mail: Marios.Zarifakis@esb.ie

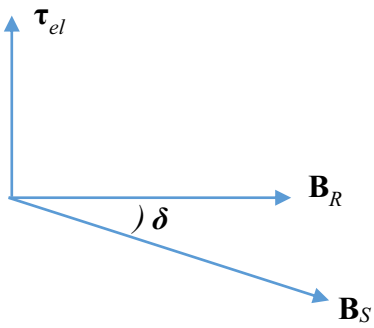

Fig. 1. The electromagnetic torque $\boldsymbol{\tau}_{el} = kB_S B_R \sin\delta$ in the air gap of the generator.

operation and the integrity of conventional generating units it is necessary to define an appropriate dynamical model which we can mathematically analyse for the purpose of calculation of the ensuing electrical and mechanical behaviour of the generator sets. Our objective being to assess the consequences for their individual components, *e.g.* the generator with its electrical windings in the rotor and stator, the turbine with its blades and the coupling to the generator.

The paper is organized as follows. We first envisage the generator-grid system as a driven damped pendulum (making large oscillations), where we suppose that the grid has infinite inertia. This leads to a torque-balance equation in the form of the equation of motion of the angle δ between the rotor and stator fields which is now no longer constant instead oscillating because of the transient disturbance. This infinite grid inertia model allows one to estimate the energy dependent frequency of the disturbance in terms of an elliptic integral as well as the response to a short impulsive change of torque due to a transient fault (trip of a generator or disconnection of a large consumer). Next, the model is generalized to a finite grid inertia (such as obtains in an isolated grid like that of the island of Ireland). The generalization leads to two coupled nonlinear pendulum-like equations for the motion of the generator-grid system whereby the system may oscillate about an equilibrium position. These equations may be solved using matrix continued fractions and the response of the generator-grid system so obtained following the sudden imposition of a set of impulses is substantially in accordance with an actual ROCOF event. This second model explicitly takes account of the fact that when reviewing the measured data, it is clear that the grid frequency also exhibits a slight oscillation in phase with the power oscillation, indicating that these two are influencing each other. Since the grid inertia in the island of Ireland is not infinite any transient disturbance will induce a rotor angle oscillation which in turn leads to a grid oscillation. Hence, the assumption that is valid for an infinite grid (model 1), namely that no feedback of the oscillation experienced by the turbine generator shaft back to the grid exists, leads us to the conclusion that the single-mass mechanical analogue is not useful when applied to grids with small inertia. Thus the main focus of our attention will be on the second model.

2 A single-mass model: equation of motion (model 1)

The dynamical equations of central importance in power system stability analysis are the rotational inertial equations of motion describing the effect of imbalance between the electromagnetic torque and the mechanical torque of the individual machines. Now during stable operation of a synchronous generator, the electromagnetic torque in the airgap between rotor and stator of the generator is equal to the mechanical torque applied by the turbine rotor to the rotor of the generator, $\tau_{el} = \tau_m$. However when a disturbance occurs, an accelerating torque which can be either positive or negative acts on the turbo shaft inertia. The turbo shaft comprises the coupled turbine and generator rotor, which during such a disturbance either accelerates or de-accelerates.

The electric currents in the stator windings of a synchronized generator create an electromagnetic field in the air gap of the generator [1]. The strength of the magnetic field $B_S = |\mathbf{B}_S|$ is constant for constant stator currents. Now, since these currents are sinusoidal the field vector $\mathbf{B}_S$ rotates about the generator axis with angular velocity $\omega_0 = 2\pi f_0$, where f_0 is the grid frequency. In a synchronous machine the rotor field vector $\mathbf{B}_R$ rotates with the same angular velocity as the stator field. The magnitude of the rotor field $B_R = |\mathbf{B}_R|$ is constant as the field is induced by a DC current. Thus, the following electromagnetic torque $\boldsymbol{\tau}_{el}$ arises in the air gap of the generator, *viz.*,

$$\boldsymbol{\tau}_{el} = k\mathbf{B}_R \times \mathbf{B}_S, \tag{1}$$

where k is a characteristic constant of the machine which depends on its geometry. Equation (1) can be rewritten as (see fig. 1)

$$\boldsymbol{\tau}_{el} = k \begin{vmatrix} \mathbf{e}_x & \mathbf{e}_y & \mathbf{e}_z \\ B_R\cos\delta_R & B_R\sin\delta_R & 0 \\ B_S\cos\delta_S & B_S\sin\delta_S & 0 \end{vmatrix} = \mathbf{e}_z k B_R B_S \sin\delta, \tag{2}$$

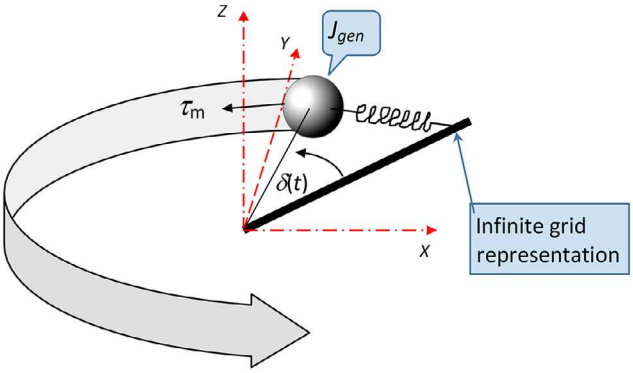

Fig. 2. Scheme with an infinite inertia of the grid.

where δ_R and δ_S are the angles between the vectors $\mathbf{B}_R$ and $\mathbf{B}_S$ and the X-axis, respectively, and $\delta = \delta_S - \delta_R$ is the angle between $\mathbf{B}_S$ and $\mathbf{B}_R$ (see fig. 1). The angle δ is called the rotor angle or in some cases the torque angle. The additional mechanical torque $\boldsymbol{\tau}_m$ is transmitted from the turbine to the generator through the coupling of the turbine rotor and the generator rotor. Now if an imbalance between the torques $\boldsymbol{\tau}_{el}$ and $\boldsymbol{\tau}_m$ exists, the net torque $\boldsymbol{\tau}_m - \boldsymbol{\tau}_{el}$ causes a rate of change of angular momentum of the generator. Consequently, the angle $\delta(t)$ between $\mathbf{B}_S$ and $\mathbf{B}_R$ either increases or decreases. The total rotational kinetic energy of the system is $\Gamma = J\dot{\theta}^2/2$, where $\theta(t) = \omega_0 t + \delta(t)$ and J is the combined moment of inertia of generator and turbine. The potential energy of the system is $\Pi = kB_S B_R[1 - \cos(\theta(t) - \omega_0 t)]$. The total energy dissipated due to the damping torque is $D = K_D(\dot{\theta}(t) - \omega_0)^2/2$. The damping torque in this case is the torque which is created by the asynchronous operation of the generator. As we are analysing the behaviour of a synchronous generator an oscillation of its frequency results in creation of a so called slip which when negative creates a mechanical torque to the shaft, when positive it creates an additional electrical torque whereby the power output is increased. Hence it only exists when the angular velocity of the generator rotor *differs* from the angular velocity of the grid. All other energy losses, like friction or thermal losses are neglected hence we have the differential equation for δ:

$$J\ddot{\delta}(t) + K_D\dot{\delta}(t) + kB_S B_R \sin\delta(t) = \tau_m,$$

or

$$\ddot{\delta}(t) + \beta\dot{\delta}(t) + \xi \sin\delta(t) = \bar{\tau}_m, \tag{3}$$

where $\beta = K_D/J$, $\xi = kB_S B_R/J$, and $\bar{\tau}_m = \tau_m/J$. This single-mass model is commonly used to analyze the dynamic response of a synchronous generator in an infinite grid [1–3]. The mechanical analogue is a *driven damped pendulum*. In accordance with eq. (3) both grid and generator initially rotate with constant rotor angle $\delta_0 = \arcsin[\tau_m/(kB_S B_R)] = \text{const.}$ (see fig. 2). The bar in fig. 2 symbolizing the grid, moves according to the grid frequency and is of *infinite* inertia, meaning that it cannot be influenced by the inertia of a single generator. In the steady-state situation both inertias, comprising the generator turbine shaft J_{gen} and the grid J_{grid} rotate in a plane horizontally about the z-axis with angular velocity ω_0 corresponding to the nominal grid-frequency of 50 Hz. However, during *transient* faults on the system like the trip of a generator or the disconnection of a large load, the grid-frequency changes. Hence the generator will experience an *additional* torque as the grid inertia alters its angular velocity. This disturbance leads to an oscillation of the rotor angle $\delta(t)$. The rotor angle oscillations result in a power output oscillation because the electrical power of a generator is determined via the rotor angle as $P_{el} = P_{\max}\sin\delta(t)$. Hence the rate of change of the grid frequency is of major importance.

If a disturbance of the motion takes place the period T of oscillations of the angle $\delta(t)$ may be estimated by considering the idealized free motion of a generator when the damping and torque τ_m are absent, *i.e.*, $\beta = 0$ and $\tau_m = 0$. The solution of eq. (3) in this case is given by (see appendix A) [4]

$$\sin[\delta(t)/2] = \sqrt{m}\,\mathrm{sn}\left[\sqrt{\xi}(t - t_0) \mid m\right], \tag{4}$$

where $\mathrm{sn}(u \mid m)$ is a Jacobian elliptic function [5] with modulus $m = \sin^2(\delta_0/2)$, δ_0 is the amplitude and t_0 is the initial time at which $\delta = \delta_0$ and $\dot{\delta} = 0$. The exact expression for the period T is given by

$$T = 4\sqrt{\frac{J}{kB_S B_R}}K(m), \tag{5}$$

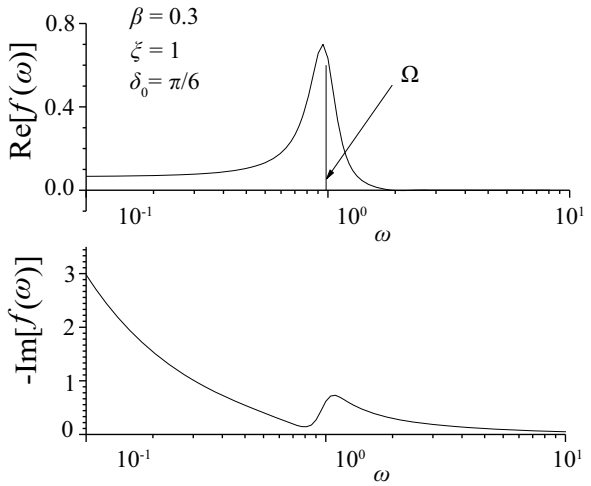

Fig. 3. Real and imaginary parts of the linear combination $f(\omega) = [\tilde{c}_{1-1}(i\omega) - \tilde{c}_{1-1}(i\omega)]/2i$ calculated by using the matrix continued fraction method (see appendix B). The frequency of free motion Ω is given by eq. (6).

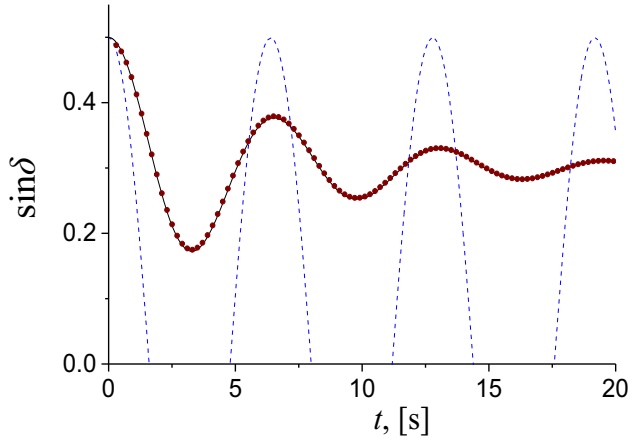

Fig. 4. Solid line: numerical solution of eq. (3) obtained by using Mathematica®. Circles: continued fraction solution of eq. (3) in the frequency domain following from the inverse Fourier transform (see appendix B) with initial conditions $\delta_0 = \pi/6$, $\dot{\delta}_0 = 0$ for the following model parameters $\xi = 1$, $\bar{\tau}_m = 0.3$, $\beta = 0.3$. Dashed line: analytical solution for $\beta = 0$, eq. (4) whereby we may estimate the period analytically.

where $K(m)$ is a complete elliptic integral of the first kind [5]. Thus the angular frequency of the periodic motion is

$$\Omega = \frac{2\pi}{T} = \frac{\pi\sqrt{kB_S B_R/J}}{2K(m)}\,. \tag{6}$$

The solution of the damped pendulum equation (3) in terms of continued fractions is given in appendix B [6]. We suppose that a disturbance of the motion occurs at the instant $t_0 = 0$ when the torque $\bar{\tau}_m$ changes from the initial value $\bar{\tau}_m^0 = \xi \sin\delta_0$ to $\bar{\tau}_m < \bar{\tau}_m^0$. Here $\delta_0 = \delta(0)$ is the initial angle. The value of δ_0 depends on the applied torque of the turbine. The initial value of $\dot{\delta}_0 = \dot{\delta}(0)$ is zero. By deriving from eq. (3) a set of differential-recurrence equations for the functions $c_{nq}(t) = \dot{\delta}^n r^q$, we can solve this set for the one-sided Fourier transforms $\tilde{c}_{nq}(i\omega)$ of $c_{nq}(t)$ via matrix continued fractions. Next, using the fast Fourier transform algorithm allows us to recover the function $c_{nq}(t)$. Having calculated $c_{nq}(t)$, we can evaluate all other functions of interest. For example, we have

$$\sin\delta(t) = \frac{c_{0-1}(t) - c_{01}(t)}{2i} \tag{7}$$

and so on. The results of such calculations for the linear combination of the one-sided Fourier transforms $\tilde{c}_{1\pm1}(i\omega)$ in the frequency domain are shown in fig. 3.

Equation (3) can also be solved numerically using Mathematica®. A comparison of the numerical and continued fraction solutions of eq. (3) is shown in fig. 4. Figure 5 shows the response of the system to a set of impulses (representing the alternating character of changes of $\bar{\tau}_m$ due to external events). This result can be compared with the measured power output of a single shaft combined cycle 400 MW synchronous generator after a real ROCOF event [1] (see fig. 6).

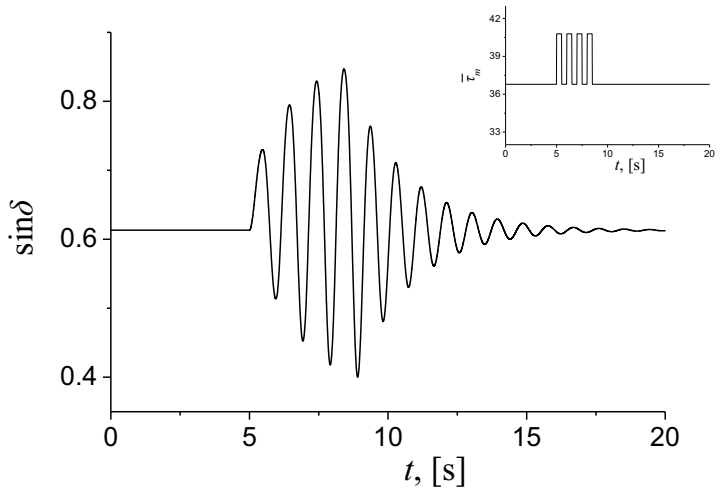

Fig. 5. Response of the system (eq. (3)) to a set of impulses of torque $\bar{\tau}_m$ for the initial conditions $\delta_0 = 0.66$, $\dot{\delta}_0 = 0$ and the following model parameters $\xi = 60$, $\beta = 1$.

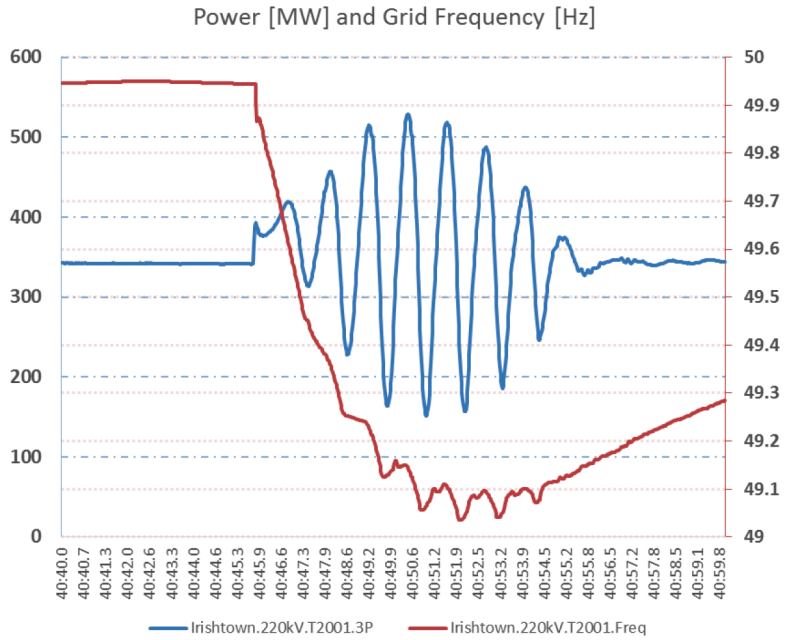

Fig. 6. Power output (blue, left scale) and grid frequency (red, right scale) of a 400 MW synchronous generator as a response of a real ROCOF event, real time in [min:sec].

The power oscillation obtained from the model (fig. 5) reproduces qualitatively well the experimentally measured oscillation of the power in fig. 6. However this model assumes infinite grid inertia, *i.e.* a fixed grid frequency. The most important feature of fig. 6 is that the grid frequency executes an oscillation in phase with the power oscillation indicating that they influence each other. Furthermore, recent observations indicate that the smaller the inertia in the grid, the more the output power of a generator oscillates. Now the grid frequency experiences such drops about 20–30 times annually. These are usually due to trips of generating stations or disconnection of a large load (which, for example, can happen when an HVDC interconnector trips while exporting electric energy from Ireland to Great Britain). Hence the ability to calculate exactly how the grid frequency behaves during such disturbances demands an approach whereby that frequency can be influenced by the transient behaviour of a generating station rather than just the ability to calculate the maximum ROCOF alone. As seen in the previous analysis, any transient disturbance can induce a rotor angle oscillation resulting in mechanical oscillations of the generator-turbine rotor. Hence, we have oscillations of the power output of the set leading to a grid oscillation and in turn this grid oscillation again influences how the turbo-set oscillates and so on. Thus the assumption that is valid for an *infinite grid*, namely, that no feedback of the oscillation experienced by the turbine generator shaft back to the grid exists, leads one to the conclusion that the single-mass model is not useful when applied to grids with *small* inertia so that we need a two-mass pendulum model with two degrees of freedom.

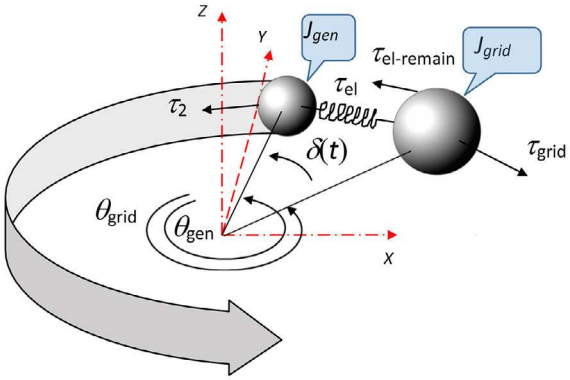

Fig. 7. Scheme with a finite inertia of the grid.

3 The two-mass pendulum (model 2)

This model, where the grid now has *finite* moment of inertia such as obtains in the isolated grid of Ireland (see fig. 7), leads to the following set of two coupled equations of motion for the generator and grid:

$$J_{\text{grid}}\ddot{\theta}_{\text{grid}} + K_D(\dot{\theta}_{\text{grid}} - \dot{\theta}_{\text{gen}}) + \tau_{el\,\max}\sin(\theta_{\text{grid}} - \theta_{\text{gen}}) = \tau_1 = \tau_{\text{grid}} - \tau_{el\text{-remain}}, \tag{8}$$

$$J_{\text{gen}}\ddot{\theta}_{\text{gen}} + K_D(\dot{\theta}_{\text{gen}} - \dot{\theta}_{\text{grid}}) + \tau_{el\,\max}\sin(\theta_{\text{gen}} - \theta_{\text{grid}}) = \tau_2 = \tau_{\text{gen}}, \tag{9}$$

where $\tau_{el\,\max}$ is the maximum electromagnetic torque in the air gap, τ_2 is the torque applied by the turbine to the generator, τ_1 is the resulting torque applied to the grid (sum of all turbine torques less the torques due to the loads and remaining generators $\tau_{el\text{-remain}}$ on the grid). Here the damping torques, characterized by the damping coefficient K_D, are those torques, which are present only when the rotor angle oscillates. In this case, the turbine controller reacts to a drop of the frequency by increasing the output of the set. It opens the valves to allow an increase of the power output. All generating units in the grid have this control behaviour. We emphasize that eqs. (8) and (9) represent a model which still has limitations, *e.g.* the energy losses due to resistances in the generators and lines are ignored.

The formal solution of eqs. (8) and (9) is given in appendix C. For the purpose of analysis of the generator and grid response to various disturbances we use below numerical solutions of eqs. (8) and (9) obtained in `Mathematica`®. At this stage one needs to point out that after a disturbance, all generators in the system increase their mechanical torque, by means of increasing the load of the turbine. This behaviour is programmed in the turbine controllers and is called primary (POR), secondary (SOR) and tertiary operating reserve (TOR). To enable one to understand the behaviour of a generator during a transient disturbance, all these torques from controllers and all the remaining generators in the power system were combined and visualised as an impulse or a set of impulses (caption in fig. 5). Figure 8 shows the response of the system (grid frequency $f_{\text{grid}} = \dot{\theta}_{\text{grid}}/(2\pi)$, generator frequency $f_{\text{gen}} = \dot{\theta}_{\text{gen}}/(2\pi)$, power output $P_{el}/P_{\max} = \sin\delta(t)$ and ROCOF $= \Delta f_{\text{grid}}/\Delta t = \Delta\dot{\theta}_{\text{grid}}/(2\pi\Delta t)$) to a set of short impulsive changes of τ_1 (as mentioned earlier representing the alternating character of changes of τ_1 due to external events such as oscillations of other generators) for different values of the inertia ratio $x = J_{\text{grid}}/J_{\text{gen}}$: $x = 7$ (column (a)), $x = 30$ (column (b)) and $x = 100$ (column (c)). Here $\delta = \theta_{\text{grid}} - \theta_{\text{gen}}$ and x is a parameter describing how much inertia lies within the transmission system. For example, for $x = 7$, the grid has 7 times as much inertia as the generator in question. The initial value of the angle δ_0 allows one to obtain a maximum initial power output which is proportional to $\sin\delta_0$ and yet allows it to still remain in the linear regime (where $\sin\delta_0 \approx \delta_0$). The recovery of the frequency to its initial (*i.e.* normal) value is accomplished by adjusting τ_1 following a perturbation. This recovery is in practice achieved by increasing the power output of those generating units remaining connected to the system. The power output increase is a function which is called primary and secondary operating reserve. Clearly, the power output (third row plots in fig. 8) qualitatively corresponds to the measurements seen in reality. Figure 8 also shows the ROCOF (fourth row) corresponding to the first row with $\Delta t = 100\,\text{ms}$. The response of the system (eqs. (8) and (9)) to an applied impulse in addition to the permanent torque τ_1 (*i.e.* a short impulsive change in τ_1) is shown in fig. 9.

Now it is important to emphasize that the numerical solution of eqs. (8) and (9) indicates that for $x = 5$ the generator would experience a pole slip as seen in fig. 9. This finding is in contradiction with the commonly used formula for ROCOF, namely

$$\frac{\mathrm{d}f}{\mathrm{d}t} = \frac{\Delta P}{P}\frac{f_0}{2H}, \tag{10}$$

where ΔP [MW] is the power change per unit machine base, P [MW] is the total power generated and H [s] is the system inertia. Equation (10) expressed via the parameters of the model, namely $2HP_N = J_{\text{grid}}\omega_0^2$ and $\Delta P \approx \Delta\tau\omega_0$,

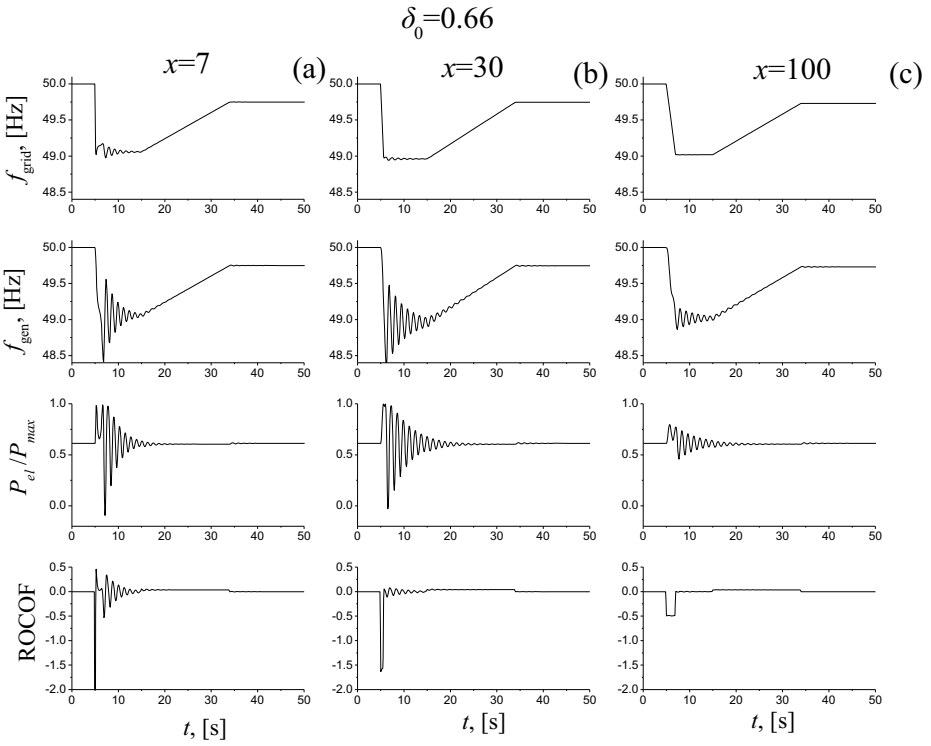

Fig. 8. Response of the generator-grid system to a short impulsive change in τ_1. The calculations correspond to the initial conditions $\delta_0 = 0.66$, $\dot{\theta}_{\mathrm{gen}}(0) = \dot{\theta}_{\mathrm{grid}}(0) = 0$ and the following parameters: $J_{\mathrm{gen}} = 71 \cdot 10^3\,\mathrm{kg \cdot m^2}$, $\beta_{\mathrm{gen}}/J_{\mathrm{gen}} = 0.42\,\mathrm{s}^{-1}$ $\beta_{\mathrm{grid}}/J_{\mathrm{grid}} = 2.8/x\,\mathrm{s}^{-1}$, and $\tau_2 = \tau_1 = 1.3 \cdot 10^6\,\mathrm{N \cdot m}$.

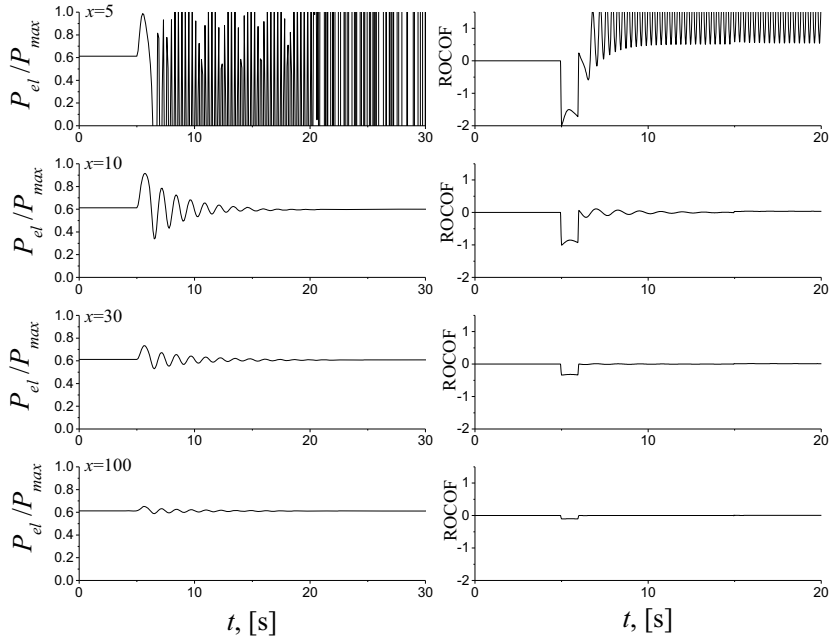

Fig. 9. The response of the system to the same additional impulse of torque $\Delta\tau_{\mathrm{grid}}$ for different values of x.

gives

$$\frac{\mathrm{d}f}{\mathrm{d}t} = \frac{\Delta P}{P}\frac{f_0}{2H} \approx \frac{\Delta P f_0}{2HP_N} = \frac{\Delta\tau\omega_0 f_0}{J_{\mathrm{grid}}\omega_0^2} = \frac{\Delta\tau}{2\pi x J_{\mathrm{gen}}}\,. \tag{11}$$

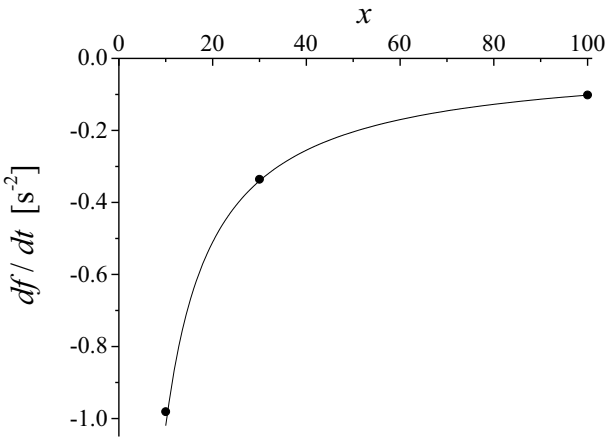

Fig. 10. $\mathrm{d}f/\mathrm{d}t$ *vs.* $x = J_{\mathrm{grid}}/J_{\mathrm{gen}}$ for $J_{\mathrm{gen}} = 71 \cdot 10^3\,\mathrm{kg}\cdot\mathrm{m}^2$, $\tau_{\mathrm{gen}} = 1.3 \cdot 10^6\,\mathrm{N}\cdot\mathrm{m}$ and $\Delta\tau_{\mathrm{grid}} = -3.5\tau_{\mathrm{gen}}$. Solid line: eq. (11). Filled circles: solution of eqs. (8) and (9).

The comparison of numerical calculations of $\mathrm{d}f/\mathrm{d}t$ *vs.* $x = J_{\mathrm{grid}}/J_{\mathrm{gen}}$ with the traditionally used eq. (11) is shown in fig. 10. Clearly good agreement exists between the numerical solution of eqs. (8) and (9) and the approximation contained in eq. (11) for $x > 10$. For values of x less than 10 one cannot use such an approximation.

4 Conclusion

We have described a viable mathematical model where the grid is postulated as a rotating mass representing a grid with decreased inertia as is obtained when it is operated *with a large amount of non-synchronous penetration*. This situation occurs in the island of Ireland and other isolated grids during times of strong penetration by (predominantly) wind turbines, etc.

Clearly, the results of the analysis highlight the potential risks when a unit is exposed to a disturbance in a system with high wind penetration and consequential low inertia. Whereas in traditional large inertia systems the oscillation steadily decreases we perceive that in systems with small inertia the stresses on the unit may also increase. Although the mechanical torques may not reach a level where one expects to see immediate crack development in a turbine generator shaft component nevertheless the magnitude of the oscillations experienced could introduce additional crack-propagation where a crack already exists.

The technical risks can be broadly associated with three driving processes:

a) Large changes in electrical power output affecting controllers such as excitation systems, power system stabilizers, turbine controller and unit controllers.
b) Large changes in the electromagnetic torque introducing critical mechanical oscillations affecting both the mechanical integrity of the generator and the turbine rotor and its components.
c) Inherent response of a unit to falling frequency such as gas compressor performance or inertial energy delivery possibly triggering a protection to disconnect the unit from the grid leading to cascade events, possibly even to a blackout of the entire electricity network.

However our major finding is that by using the solutions set out in the equations describing the double pendulum, one may define the safe operational limits for synchronously connected generators, in a small inertia system, thereby gaining a better understanding of how low inertia systems react during transient disturbances and thus maximizing the quantity of renewable energy which may be generated.

We thank Dr W.J. Dowling for a critical reading of the paper and useful comments and suggestions.

Appendix A. Solution of free pendulum equation

For $\beta = \bar{\tau}_m = 0$, we rearrange eq. (3) as

$$2\dot{\delta}(t)\ddot{\delta}(t) + 2\xi\dot{\delta}(t)\sin\delta(t) = \frac{\mathrm{d}}{\mathrm{d}t}\left[\dot{\delta}^2(t) - 2\xi\cos\delta(t)\right] = 0. \tag{A.1}$$

Thus we have from eq. (A.1)

$$\dot{\delta}^2(t) = 2\xi\left[\cos\delta(t) - \cos\delta_0\right] = 4\xi\left[\sin^2\frac{\delta_0}{2} - \sin^2\frac{\delta(t)}{2}\right], \tag{A.2}$$

or

$$\frac{\mathrm{d}\delta}{2\sqrt{\sin^2(\delta_0/2) - \sin^2(\delta/2)}} = \sqrt{\xi}\mathrm{d}t, \tag{A.3}$$

where δ_0 is an integration constant. By integrating eq. (A.3) with the initial condition $\delta(t_0) = 0$, we have

$$\int_0^{\delta} \frac{\mathrm{d}(\delta/2)}{\sqrt{m - \sin^2(\delta/2)}} = \int_0^{m^{-1/2}\sin\delta/2} \frac{\mathrm{d}t}{\sqrt{(1-mt^2)(1-t^2)}} = \sqrt{\xi}(t - t_0), \tag{A.4}$$

where $m = \sin^2\delta_0/2$, so yielding eq. (4).

Appendix B. Matrix continued fraction solution of damped pendulum equation

In the general case, we have for the function $c_{nq}(t) = \dot{\delta}^n r^q$ with $r = e^{-i\delta(t)}$

$$\begin{aligned}\frac{\mathrm{d}}{\mathrm{d}t}c_{nq}(t) &= n\dot{\delta}^{n-1}r^q\ddot{\delta} - iq\dot{\delta}^{n+1}r^q \\ &= -iqc_{n+1q}(t) - n\dot{\delta}^{n-1}r^q\left[\beta\dot{\delta}(t) + \xi\sin\delta(t) - \bar{\tau}_m\right].\end{aligned} \tag{B.1}$$

Here we substitute $\ddot{\delta}(t) = -\beta\dot{\delta}(t) - \xi\sin\delta(t) + \bar{\tau}_m$ from eq. (3). By using $\sin\delta(t) = (r^{-1} - r)/2i$ in eq. (B.1), we have the following differential-recurrence relation for $c_{nq}(t)$:

$$\frac{\mathrm{d}}{\mathrm{d}t}c_{nq}(t) = -\beta nc_{nq}(t) - iqc_{n+1q}(t) - \frac{in}{2}\left[\xi c_{n-1q+1}(t) + 2i\bar{\tau}_m c_{n-1q} - \xi c_{n-1q-1}(t)\right]. \tag{B.2}$$

By introducing infinite column vectors,

$$\mathbf{C}_0(t) = 0, \qquad \mathbf{C}_n(t) = \begin{pmatrix} \vdots \\ c_{n-1-2}(t) \\ c_{n-1-1}(t) \\ c_{n-10}(t) \\ c_{n-11}(t) \\ c_{n-12}(t) \\ \vdots \end{pmatrix} \quad (n > 0), \tag{B.3}$$

the differential-recurrence equations (B.2) can be transformed into the tri-diagonal matrix form

$$\frac{\mathrm{d}}{\mathrm{d}t}\mathbf{C}_n(t) = \mathbf{Q}_n^-\mathbf{C}_{n-1}(t) + \mathbf{Q}_n\mathbf{C}_n(t) + \mathbf{Q}_n^+\mathbf{C}_{n+1}(t). \tag{B.4}$$

Here the matrices $\mathbf{Q}_n$ and $\mathbf{Q}_n^{\pm}$ are

$$\mathbf{Q}_n = -\beta(n-1)\mathbf{I}, \tag{B.5}$$

$$\mathbf{Q}_n^{+} = -i \begin{pmatrix} \ddots & \ddots & \ddots & & \\ \ddots & -1 & 0 & \ddots & \\ \ddots & 0 & 0 & 0 & \ddots \\ & \ddots & 0 & 1 & \ddots \\ & & \ddots & \ddots & \ddots \end{pmatrix}, \tag{B.6}$$

$$\mathbf{Q}_n^{-} = -(n-1) \begin{pmatrix} \ddots & \ddots & \ddots & & \\ \ddots & \bar{\tau}_m & i\xi/2 & \ddots & \\ \ddots & -i\xi/2 & \bar{\tau}_m & i\xi/2 & \ddots \\ & \ddots & -i\xi/2 & \bar{\tau}_m & \ddots \\ & & \ddots & \ddots & \ddots \end{pmatrix}, \tag{B.7}$$

and $\mathbf{I}$ is the unit matrix of infinite dimension.

Equation (B.4) is solved by the matrix continued fraction method [6,7]. On considering the initial conditions $\delta(0) = \delta_0$ and $\dot{\delta}(0) = 0$ and taking the Laplace transform of eq. (B.4), we obtain the matrix recurrence relations for the Laplace transforms $\tilde{\mathbf{C}}_n(s)$:

$$-s\tilde{\mathbf{C}}_1(s) + \mathbf{Q}_1^{+}\tilde{\mathbf{C}}_2(s) = -\mathbf{C}_1(0), \tag{B.8}$$

$$\mathbf{Q}_n^{-}\tilde{\mathbf{C}}_{n-1}(s) + (\mathbf{Q}_n - s\mathbf{I})\,\tilde{\mathbf{C}}_n(s) + \mathbf{Q}_n^{+}\tilde{\mathbf{C}}_{n+1}(s) = 0 \quad (n > 1), \tag{B.9}$$

where

$$\tilde{\mathbf{C}}_n(s) = \int_0^{\infty} \mathbf{C}_n(t)e^{-st}\mathrm{d}t. \tag{B.10}$$

Here we have noted that

$$\mathbf{C}_1(0) = \begin{pmatrix} \vdots \\ e^{2i\delta_0} \\ e^{i\delta_0} \\ 1 \\ e^{-i\delta_0} \\ e^{-2i\delta_0} \\ \vdots \end{pmatrix}, \qquad \mathbf{C}_n(0) = 0, \quad n > 2.$$

We seek the solution of the linear eqs. (B.8) and (B.9) as

$$\tilde{\mathbf{C}}_n(s) = \boldsymbol{\Delta}_n\mathbf{Q}_n^{-}\tilde{\mathbf{C}}_{n-1}(s) + \mathbf{R}_n, \tag{B.11}$$

where $\boldsymbol{\Delta}_n$ is the matrix continued fraction defined by the recurrence equation

$$\boldsymbol{\Delta}_n = \left[s\mathbf{I} - \mathbf{Q}_n - \mathbf{Q}_n^{+}\boldsymbol{\Delta}_{n+1}\mathbf{Q}_{n+1}^{-}\right]^{-1}, \tag{B.12}$$

which allows us to represent $\boldsymbol{\Delta}_n$ as an infinite matrix continued fraction [7]. Substituting eq. (B.11) into eqs. (B.8) and (B.9) yields

$$\left[s\mathbf{I} - \mathbf{Q}_1 - \mathbf{Q}_1^{+}\boldsymbol{\Delta}_2\mathbf{Q}_2^{-}\right]\mathbf{R}_1 = \mathbf{C}_1(0) + \mathbf{Q}_1^{+}\mathbf{R}_2, \tag{B.13}$$

$$\left[s\mathbf{I} - \mathbf{Q}_n - \mathbf{Q}_n^{+}\boldsymbol{\Delta}_{n+1}\mathbf{Q}_{n+1}^{-}\right]\mathbf{R}_n = \mathbf{Q}_n^{+}\mathbf{R}_{n+1} \quad (n > 1). \tag{B.14}$$

Equations (B.13) and (B.14) can be solved exactly for the desired *particular solutions* $\mathbf{R}_n$ in terms of the matrix continued fraction $\boldsymbol{\Delta}_1$:

$$\mathbf{R}_1 = \boldsymbol{\Delta}_1 \mathbf{C}_1(0), \qquad \mathbf{R}_n = 0 \quad (n > 1). \tag{B.15}$$

Substituting eq. (B.15) into eq. (B.11) yields the matrix continued-fraction solution of eqs. (B.8) and (B.9) for the Laplace transforms $\tilde{\mathbf{C}}_n(s)$ [7]

$$\tilde{\mathbf{C}}_1(s) = \boldsymbol{\Delta}_1 \mathbf{C}_1(0), \tag{B.16}$$

$$\tilde{\mathbf{C}}_n(s) = \boldsymbol{\Delta}_n \mathbf{Q}_n^- \tilde{\mathbf{C}}_{n-1}(s) = \boldsymbol{\Delta}_n \mathbf{Q}_n^- \boldsymbol{\Delta}_{n-1} \mathbf{Q}_{n-1}^- \dots \boldsymbol{\Delta}_1 \mathbf{C}_1(0) \quad (n > 1). \tag{B.17}$$

The matrix continued fraction solution we have obtained is very convenient for the purpose of computation (various algorithms for calculating matrix continued fractions are discussed in refs. [6] and [7]). As far as the calculation of the infinite matrix continued fraction $\boldsymbol{\Delta}_n$ is concerned, we approximated it by some matrix continued fraction of finite order (by putting $\mathbf{Q}_{n+1} = 0$ at some $n = K$). At the same time, we confined the dimensions of the matrices $\mathbf{Q}_n$ and $\mathbf{Q}_n^{\pm}$ to some finite number $2M + 1$. Both K and M depend on the model parameters and must be chosen taking account of the desired degree of accuracy of the calculation. The calculation of the time-dependent functions $c_{nq}(t)$ can be then accomplished using the Fast Fourier Transform (FFT) algorithm as

$$\begin{aligned} c_{nq}(t) &\approx \frac{1}{\pi} \operatorname{Re} \left[\int_0^{\Omega'(N-1)} \tilde{c}_{nq}(i\omega) e^{i\omega t} \mathrm{d}\omega \right] \\ &= \frac{\Omega'}{\pi} \operatorname{Re} \left[\sum_{s=1}^{N} \tilde{c}_{nq} \left(i\Omega'(s-1) \right) e^{i\Omega'(s-1)t} \right], \end{aligned} \tag{B.18}$$

or

$$\begin{aligned} c_{nq}\left(T(r-1)\right) &= \frac{\Omega'}{\pi} \operatorname{Re} \left[\sum_{s=1}^{N} \tilde{c}_{nq} \left(i\Omega'(s-1) \right) e^{i\Omega' T(s-1)(r-1)} \right] \\ &(r = 1, 2, \dots, N), \end{aligned} \tag{B.19}$$

where

$$\Omega' = \frac{2\pi}{NT}, \quad N = 2^k. \tag{B.20}$$

Appendix C. Matrix continued fraction solution of eqs. (8) and (9)

Equations (8) and (9) can be rewritten as

$$\ddot{\theta}_i + \beta_i(\dot{\theta}_i - \dot{\theta}_j) + \xi_i \sin\left(\theta_i - \theta_j\right) = \bar{\tau}_i \quad (i = 1, 2 \text{ and } j = 2, 1), \tag{C.1}$$

where $\theta_1 = \theta_{\mathrm{grid}}$, $\beta_1 = K_D^1/J_{\mathrm{grid}}$, $\xi_1 = \tau_{el\,\max}/J_{\mathrm{grid}}$, $\theta_2 = \theta_{\mathrm{gen}}$, $\beta_2 = K_D^2/J_{\mathrm{gen}}$, $\xi_2 = \tau_{el\,\max}/J_{\mathrm{gen}}$, $\bar{\tau}_1 = \tau_1/J_{\mathrm{grid}}$ and $\bar{\tau}_2 = \tau_2/J_{\mathrm{grid}}$.

Now we introduce

$$c_{n_2 q_2}^{n_1 q_1} = \dot{\theta}_1^{n_1} \dot{\theta}_2^{n_2} r_1^{q_1} r_2^{q_2}, \quad n = 0, 1, 2 \dots, \quad q = 0, \pm 1, \pm 2 \dots, \tag{C.2}$$

where $r_i = e^{-i\theta_i(t)}$. Then, noting eqs. (C.1) and (C.2), we have

$$\begin{aligned} \frac{\mathrm{d}}{\mathrm{d}t} c_{n_2 q_2}^{n_1 q_1} &= -\left(\beta_1 n_1 + \beta_2 n_2\right) c_{n_2 q_2}^{n_1 q_1} + \beta_1 n_1 c_{n_2+1 q_2}^{n_1-1 q_1} + \beta_2 n_2 c_{n_2-1 q_2}^{n_1+1 q_1} - i q_1 c_{n_2 q_2}^{n_1+1 q_1} - i q_2 c_{n_2+1 q_2}^{n_1 q_1} \\ &+ \bar{\tau}_1 n_1 c_{n_2 q_2}^{n_1-1 q_1} + \frac{i}{2} \xi_1 n_1 \left(c_{n_2 q_2+1}^{n_1-1 q_1-1} - c_{n_2 q_2-1}^{n_1-1 q_1+1} \right) + \bar{\tau}_2 n_2 c_{n_2-1 q_2}^{n_1 q_1} + \frac{i}{2} \xi_2 n_2 \left(c_{n_2-1 q_2-1}^{n_1 q_1+1} - c_{n_2-1 q_2+1}^{n_1 q_1-1} \right). \end{aligned} \tag{C.3}$$

Thus on introducing column vectors $\mathbf{C}_n(t)$ defined as

$$\mathbf{C}_1(t) = \left(\mathbf{c}_{00}\right), \qquad \mathbf{C}_2(t) = \begin{pmatrix} \mathbf{c}_{10} \\ \mathbf{c}_{01} \end{pmatrix}, \dots, \qquad \mathbf{C}_n(t) = \begin{pmatrix} \mathbf{c}_{n-10} \\ \mathbf{c}_{n-21} \\ \vdots \\ \mathbf{c}_{0n-1} \end{pmatrix}, \tag{C.4}$$

where the subvectors are

$$\mathbf{c}_{n_1n_2}(t)=\begin{pmatrix}\vdots\\ c_{n_22}^{n_1-1}(t)\\ c_{n_21}^{n_10}(t)\\ c_{n_20}^{n_11}(t)\\ c_{n_2-1}^{n_12}(t)\\ \vdots\end{pmatrix}, \tag{C.5}$$

it follows that the differential-recurrence equation (C.3) can be transformed into the matrix three-term recurrence equation (B.4), namely,

$$\frac{\mathrm{d}}{\mathrm{d}t}\mathbf{C}_n(t)=\mathbf{Q}_n^-\mathbf{C}_{n-1}(t)+\mathbf{Q}_n\mathbf{C}_n(t)+\mathbf{Q}_n^+\mathbf{C}_{n+1}(t), \tag{C.6}$$

where the matrices $\mathbf{Q}_n$ and $\mathbf{Q}_n^{\pm}$ are given by

$$\mathbf{Q}_n=-\beta_1\begin{pmatrix}(n-1)\mathbf{I} & (n-1)\mathbf{I} & \mathbf{0} & \cdots & \mathbf{0}\\ \mathbf{0} & (n-2)\mathbf{I} & (n-2)\mathbf{I} & \ddots & \vdots\\ \mathbf{0} & \ddots & \ddots & \ddots & \mathbf{0}\\ \vdots & \ddots & \mathbf{0} & \mathbf{I} & \mathbf{I}\\ \mathbf{0} & \cdots & \mathbf{0} & \mathbf{0} & \mathbf{0}\end{pmatrix}-\beta_2\begin{pmatrix}\mathbf{0} & \mathbf{0} & \mathbf{0} & \cdots & \mathbf{0}\\ \mathbf{I} & \mathbf{I} & \mathbf{0} & \ddots & \vdots\\ \mathbf{0} & \ddots & \ddots & \ddots & \mathbf{0}\\ \vdots & \ddots & (n-2)\mathbf{I} & (n-2)\mathbf{I} & \mathbf{0}\\ \mathbf{0} & \cdots & \mathbf{0} & (n-1)\mathbf{I} & (n-1)\mathbf{I}\end{pmatrix}, \tag{C.7}$$

$$\mathbf{Q}_n^+=-i\begin{pmatrix}\mathbf{q}^+ & \mathbf{q}_+ & \mathbf{0} & \cdots & \mathbf{0}\\ \mathbf{0} & \mathbf{q}^+ & \mathbf{q}_+ & \ddots & \vdots\\ \vdots & \ddots & \ddots & \ddots & \mathbf{0}\\ \mathbf{0} & \cdots & \mathbf{0} & \mathbf{q}^+ & \mathbf{q}_+\end{pmatrix}, \tag{C.8}$$

$$\mathbf{Q}_n^-=\begin{pmatrix}(n-1)\mathbf{q}^- & \mathbf{0} & \cdots & \mathbf{0}\\ \mathbf{q}_- & (n-2)\mathbf{q}^- & \ddots & \vdots\\ \mathbf{0} & 2\mathbf{q}_- & \ddots & \mathbf{0}\\ \vdots & \ddots & \ddots & \mathbf{q}^-\\ \mathbf{0} & \cdots & \mathbf{0} & (n-1)\mathbf{q}_-\end{pmatrix}, \tag{C.9}$$

where

$$\mathbf{q}^+=\begin{pmatrix}-q_{\max}+1 & 0 & \cdots & 0\\ 0 & -q_{\max}+2 & \ddots & \vdots\\ \vdots & \ddots & \ddots & 0\\ 0 & \cdots & 0 & q_{\max}\end{pmatrix},\qquad \mathbf{q}_+=\begin{pmatrix}q_{\max} & 0 & \cdots & 0\\ 0 & q_{\max}-1 & \ddots & \vdots\\ \vdots & \ddots & \ddots & 0\\ 0 & \cdots & 0 & -q_{\max}+1\end{pmatrix} \tag{C.10}$$

$$\mathbf{q}^-=\begin{pmatrix}\bar{\tau}_1 & -i\xi_1/2 & \cdots & 0\\ i\xi_1/2 & \bar{\tau}_1 & \ddots & \vdots\\ \vdots & \ddots & \ddots & -i\xi_1/2\\ 0 & \cdots & i\xi_1/2 & \bar{\tau}_1\end{pmatrix},\qquad \mathbf{q}_-=\begin{pmatrix}\bar{\tau}_2 & i\xi_2/2 & \cdots & 0\\ -i\xi_2/2 & \bar{\tau}_2 & \ddots & \vdots\\ \vdots & \ddots & \ddots & i\xi_2/2\\ 0 & \cdots & -i\xi_2/2 & \bar{\tau}_2\end{pmatrix}, \tag{C.11}$$

and $\mathbf{I}$ is a unit matrix with dimension $2q_{\max}$ (here we have confined the dimensions of the matrices $\mathbf{q}^{\pm}$ and $\mathbf{q}_{\pm}$ to some finite number $2q_{\max}$).

Using the Laplace transformation, eq. (C.6) can be reduced to the matrix recurrence relations for the Laplace transforms $\tilde{\mathbf{C}}_n(s)$, eqs. (B.8) and (B.9), where

$$\mathbf{C}_1(0) = \begin{pmatrix} \vdots \\ c_{02}^{0-1}(0) \\ c_{01}^{00}(0) \\ c_{00}^{01}(0) \\ c_{0-1}^{02}(0) \\ \vdots \end{pmatrix}, \tag{C.12}$$

$c_{0q_2}^{0q_1}(0) = e^{-i(q_1\theta_1(0)+q_2\theta_2(0))}$, and $\mathbf{C}_n(0) = 0$ for $n = 2, 3, \ldots$, because $\dot{\theta}_1(0) = \dot{\theta}_2(0) = 0$. Then by invoking the general method for solving the matrix recurrence equations [6], we have the matrix continued fraction solution, eq. (B.16). The calculation of the time-dependent functions $c_{n_2q_2}^{n_1q_1}(t)$ can be then accomplished using the FFT algorithm.

Finally, the following properties of eqs. (8) and (9) can be useful in practical applications. First by adding eqs. (8) and (9), we have

$$J_{\text{grid}}\ddot{\theta}_{\text{grid}} + J_{\text{gen}}\ddot{\theta}_{\text{gen}} = \tau_1 + \tau_2. \tag{C.13}$$

Next writing eqs. (8) and (9) in the form of eq. (C.1) and subtracting the second equation from the first equation, we have

$$\ddot{\theta}_1 - \ddot{\theta}_2 + (\beta_1 + \beta_2)\left(\dot{\theta}_1 - \dot{\theta}_2\right) + (\xi_1 + \xi_2)\sin(\theta_1 - \theta_2) = \bar{\tau}_1 - \bar{\tau}_2. \tag{C.14}$$

Equation (C.14) is identical in form to eq. (3) thus it can be solved in a similar way using matrix continued fraction solution of the damped pendulum equation (see appendix B). However, the difference is that now the grid dynamics are influenced by the generator in accordance with eq. (C.13) and the grid does not oscillate anymore with a constant frequency ω_0 as in a grid with infinite inertia. However we still need to integrate eq. (C.13) twice and combine it with the continued fraction solution of eq. (C.14) in order to determine the overall dynamics of the system.

References

1. P. Kundur, *Power system stability and control*, in *The EPRI Power System Engineering Series* (McGraw Hill Inc., NY, 1994).
2. M. Zarifakis, W.T. Coffey, *Impact of elevated Rate of Change of Frequency (RoCoF) on conventional power generation plant in the Island of Ireland*, VGB PowerTech (8/2014).
3. M. Zarifakis, W.T. Coffey, *Transient Stability of conventional power generating stations during times of high wind penetration*, in *Arbeitskreis Energie, Vortraege auf der DPG Fruehjahrstagung in Berlin 2015* (9/2015).
4. E.T. Whittaker, G.N. Watson, *A Course of Modern Analysis*, 4th edition (Cambridge University Press, London, 1927).
5. M. Abramowitz, I.A. Stegun (Editors), *Handbook of Mathematical Functions* (Dover, New York, 1972).
6. W.T. Coffey, Yu.P. Kalmykov, *The Langevin Equation*, 4th edition (World Scientific, Singapore, 2017).
7. H. Risken, *The Fokker-Planck Equation*, 2nd edition (Springer, Berlin, 1989).